Journal of Molecular Structure 1233 (2021) 130027

Contents lists available at ScienceDirect

Journal of Molecular Structure

journal homepage: www.elsevier.com/locate/molstr

Conformational analysis for infrared spectroscopy and theoretical calculations of some 2-bromo-2-propyl 2-aryl-acetates, ibuprofen and naproxen analogs

Ana Carolina Abbud Hanna Roque, Daniel de Carvalho Santos, Marcelo Mota Reginato, Adriana Karla Cardoso Amorim Reis*

Department of Chemistry, Institute of Environmental, Chemical and Pharmaceutical Sciences–Federal University of São Paulo, Rua Professor Arthur Riedel, 275, CEP: 09972-270, Diadema Brazil

ARTICLE INFO

Article history:
Received 15 September 2020
Revised 9 January 2021
Accepted 26 January 2021
Available online 1 February 2021

Keywords:
2-Bromo-2-propyl 2-aryl-acetate
Conformational analysis
Infrared spectroscopy
Theoretical calculations
Natural bond orbital

ABSTRACT

Conformational analysis of new *para*–substituted 2-bromo-2-propyl 2-aryl-acetates (Y = H, OMe, Cl, and NO_2) (R1), ibuprofen (R2), and naproxen (R3) analogs using infrared (IR) spectroscopy and theoretical calculations was performed to determine the preferential conformers of these compounds in solvents with increasing polarity (CCl_4, CH_3Cl, and CH_3CN). The aryl-bromo-esters were synthesized via the coupling reactions of 2-bromo-2-methylpropan-1-ol and the corresponding carboxylic acids, with good yields (~36–70%). The IR spectra showed that these compounds presented only one conformation, and the experimental data were supported by the theoretical results obtained by density functional theory (DFT) calculations using the 6311+G (2df, 2p) basis set. The calculations revealed that all the studied compounds presented two stable geometric conformations, which agrees with the data obtained experimentally in CCl_4. Theses conformers are stabilized by intramolecular hydrogen bonds. However, the orbital interaction calculations using the natural bond orbital (NBO) method showed that the $\eta_O \rightarrow \sigma^*_{C\text{-}C}$, $\eta_O \rightarrow \sigma^*_{C\text{-}O}$, $\eta_O \rightarrow \sigma^*_{C\text{-}O}$ and $\eta_O \rightarrow \pi^*_{C\text{-}O}$ hyper-conjugations are the main interactions that stabilize the conformations. The compounds preferentially adopt the *anti*-conformation because the steric effect between the *gauche* bromo and oxygen atoms overrides the hyper-conjugative interactions, in addition to the stabilizing $\sigma_{C\text{-}H} \rightarrow \sigma^*_{C\text{-}Br}$ interactions in the conformers.

1. Introduction

Nonsteroidal anti-inflammatory drugs (NSAIDs) are the most widely prescribed and used for reducing pain, fever, and inflammation. [1] The pharmacological effects of NSAIDs arise from the inhibition of a membrane enzyme called cyclooxygenase (COX), which is involved in prostaglandin biosynthesis. [2] These NSAIDs competitively inhibit cyclooxygenase enzymes, which are primarily responsible for the conversion of arachidonic acid into prostaglandins in inflammatory processes. [3]

The discovery of two isoforms COX-1 and COX-2 in 1990 helped scientists understand the side-effects of NSAIDs. [4] The major drawback of long-term use of NSAIDs is their gastrointestinal (GI) toxicity, which arises from the inhibition of COX-1 activity and includes upper GI irritation, ulceration, dyspepsia, bleeding, and in some cases, death. [2,4,5] Recently, considerable attention has been directed towards the development of reversible derivatives, such as prodrugs and mutual prodrugs, via chemical modifications. Chemical modification or derivatization temporarily masks the acidic group of NSAIDs and appears to be a promising and fruitful method for reducing or preventing the GIT toxicity via the local insult mechanism. [6–9]

Most prodrugs from NSAIDs have been synthesized by derivatization of the free carboxylic group (-COOH) of the NSAID. [8,9] Among the various types of prodrugs, esters and amides are the most common. Many researchers have reported that the conversion of the carboxylic group of NSAIDs to amide functional groups increases their selectivity towards COX-2 and helps in decreasing the GI toxicity of the parent drug. [10]

For the ester derivatives, the authors proposed that hydrolysis of the synthesized prodrugs probably occurs via cleavage of the ester bond by esterase in the intestine, but not in the stomach where it was hypothesized to remain as an intact molecule. Thus, the gastric side-effects produced by NSAIDs are prevented by the ester derivatives. [10,11]

* Corresponding author at: 275, CEP: 09972-270, Diadema, São Paulo, Brazil.
E-mail address: adriana.amorim@unifesp.br (A.C.A.H. Roque).

https://doi.org/10.1016/j.molstruc.2021.130027
0022-2860/

The stable conformations of the NSAID aryl acetic amfenac (2-amino-3-benzoylphenylacetic acid) and its 19 substituted derivatives were studied to correlate their biological activities with structural parameters. The geometries of amfenac in the neutral and anionic forms were totally optimized, based on standard geometries and crystallographic data, using semiempirical AM1 and MNDO quantum-mechanical methods. The conformational analysis shows the existence of a rigid structure for rotations of the acetic acid chain and the central carbonyl group around the bonds with the phenylamine ring, whereas the carboxyl group and phenyl ring of the benzoyl group can rotate almost freely. [12]

NSAIDs block proteinoid biosynthesis by inhibiting prostaglandin H2 synthase (EC 1.14.99.1) in either rapidly reversible competitive or slow tight-binding mode. These different modes of inhibition correlate with clinically important differences in the isoform selectivity. Hypotheses have been advanced to explain the different inhibition kinetics, but no structural data have been available to test them. The crystal structures of prostaglandin H2 synthase-1 show that the enzyme forms complexes with the inhibitors ibuprofen, methyl flurbiprofen, flurbiprofen, and alclofenac with distances of 2.6–2.75 Å. These structures allow direct comparison of the enzyme complexes with reversible competitive inhibitors (ibuprofen and methyl flurbiprofen) and slow tight-binding inhibitors (alclofenac and flurbiprofen). The four inhibitors bind to the same site and adopt similar conformations. In all the four complexes, the enzyme structure remains essentially unchanged, exhibiting only minimal differences in the inhibitor binding site. These results strongly oppose the hypotheses explaining the difference between slow tight-binding and fast reversible competitive inhibition by invoking global conformational differences or different inhibitor binding sites. [13]

Modeling studies suggest that while both the R-(R)- and R-(S)-stereoisomers of the indomethacin ethanol-amide derivative can be well accommodated in the binding site, the R-(R)-isomers must adopt an energetically strained conformation compared to the R-(S)-isomers to form a comparable set of hydrogen bonds and van der Waals interactions with the enzyme. [14]

The structural and conformational investigations were performed experimentally in solution via NMR analysis of common flexible salicylate and 2-aryl propionic acid NSAIDs by using a combination of RDCs in PBLG-based weakly ordering liquid-crystalline solvents, along with the AP-DPD theoretical approach. By applying this methodology, conformational descriptions have been obtained for all the studied drugs from the simplest cases of diflunisal and phenyl salicylic acid (which is characterized by a single internal rotation), to the more complex cases with more internal torsions, i.e., naproxen, flurbiprofen, ibuprofen, and ketoprofen. The AP-DPD theoretical model is a solid approach for treating the experimental data for highly oriented molecules with no more than two rotations and weakly oriented drug molecules characterized by more complex conformational flexibilities. An interesting aspect of the AP-DPD strategy is that for a given molecule, it is possible to treat noncoupled rotations of the various molecular fragments and combine the results to describe the entire molecule. [15]

The ibuprofen derivative 5-(1-(4-isobutylphenyl)ethyl)-1,3,4-thiadiazol-2-amine hydrochloride is prepared by cyclization of ibuprofen with thiosemicarbazide in the presence of $POCl_3$. The compound crystallizes in the triclinic system with space group P-1 as discrete cations and chloride anions with two enantiomers in the asymmetric unit. Full vibrational analysis of the Fourier-transform infrared (FT-IR) and Fourier-transform Raman (FT-Raman) spectra has been performed in conjunction with quantum chemical calculations. The experimental data are consistent with the presence of the thiadiazole NH protonated form in the solid phase. The observation of the $\nu_{(N\text{-}N)}$ and $\delta_{(C\text{-}N\text{-}N)}$ normal modes as strong signals in the IR and Raman spectra at 1189 (1180 cm^{-1}) and 774 cm^{-1}, respectively, suggests an N-N bond with partial double-bond character in the thiadiazole moiety, consistent with the computed results at the B3LYP/6-311++G(d,p) level of approximation. The NBO analysis showed that the sulfur lone pair and the exocyclic amine nitrogen lone pair orbitals both contributed to strong resonance interactions with the adjacent $\pi^*_{(N=C)}$ antibonding orbital of the protonated thiadiazole group. [16]

Previously, a conformational study of new S-nitrosothiol esters, para–substituted S-nitrosothiol derivatives, 2-methyl-2-(sulfanyl)propyl phenylacetates, ibuprofen derivatives, 2-(4-isobutylphenyl)propanoato, and a derivative of naproxen 2-(4-isobutylphenyl)-propanoate with 2-methyl-l-2-(nitrososulfanyl)propyl was performed using IR spectroscopy in solvents with increasing polarity, combined with theoretical calculations, to determine the preferential conformers and the potential of these compounds for nitric oxide (NO) release. The IR spectra showed that these compounds present only one anticlinal (ac) geometric conformation, and the experimental data were supported by the theoretical results obtained by density functional theory (DFT) calculations using the 6311+G (2df, 2p) basis set. The calculation of the orbital interactions using the NBO method showed that the $n_{O(NO)} \rightarrow \sigma_{(SN)*}$ hyperconjugative interaction increased the S–N bond length, and strong $n_S \rightarrow \pi_{(NO)*}$ interaction and electronic delocalization induced partial π character into the S–N bond, which increased the capacity for NO release from SNO-ESTERS. [17]

In this study, we synthesize the S-nitrosothiols 2-methyl-2-(nitroso-sulfanyl) propyl-phenylacetate-para-substituted **R1**, 2-methyl-2-(nitrosothio)-propyl-2-(4-isobutylphenyl)-propanoate **R2**, and 2-methyl-2-(nitrosothio)propyl-2-(6-methoxynaphthalen-2-yl)propanoate **R3** (derivatives of ibuprofen and naproxen, respectively). A conformational study of the compounds is performed using IR spectroscopy and theoretical calculations. This combination of experimental and theoretical approaches enables us to determine the most stable conformation that these molecules can assume in relation to the carbonyl group. These compounds are used as precursors of a series of novel substituted *N*-benzylamide NSAID conjugates that are synthesized via unimolecular nucleophilic substitution reactions.

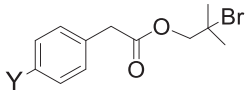

R1 (Y= OMe, H, Cl e NO_2)

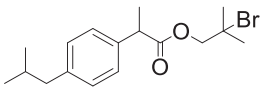

R2

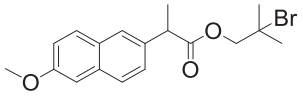

R3

2. Materials and methods

2.1. Synthesis of aryl-bromo-esters

The aryl-bromo-esters (**R1–R3**) were prepared from the coupling reaction of intermediate **2**, which was obtained from the reaction of compound **1** with $LiAlH_4$, which led to the reduction of the ester group to the alcohol (**2**) with the corresponding carboxylic acids [18]. The aryl-bromo-esters **R1–R3** were obtained in moderate-to-good yields (36–70%) using the method in Scheme 1.

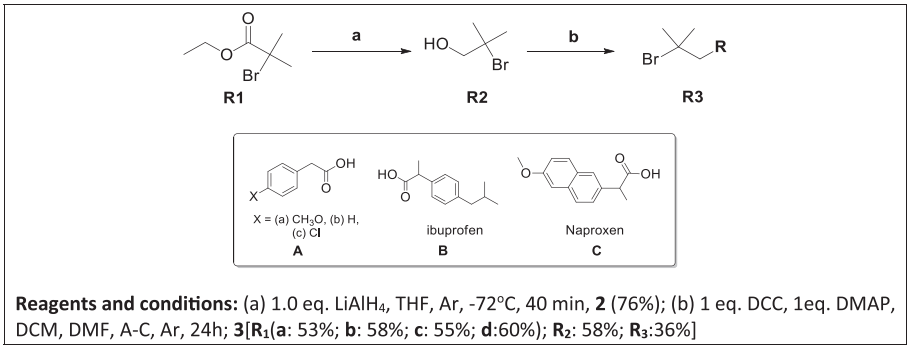

Reagents and conditions: (a) 1.0 eq. $LiAlH_4$, THF, Ar, -72°C, 40 min, **2** (76%); (b) 1 eq. DCC, 1eq. DMAP, DCM, DMF, A-C, Ar, 24h; **3**[R_1(**a**: 53%; **b**: 58%; **c**: 55%; **d**:60%); R_2: 58%; R_3:36%]

Scheme 1. Synthesis of Aryl-bromo-esters (**R1**-**R3**).

Table 1
Frequencies (ν, cm^{-1}) and intensity ratios of carbonyl stretching bands (P, %) in the infrared spectrum for the compounds 2-bromo-2-methylpropyl-2-aryl-acetate-*para*-substituted R1(Y = H, OMe, Cl and NO_2), 2-bromo-2-methylpropyl 2-(4-isobutyl-phenyl)propanoate (derivative of Ibuprofen) R2 and 2-bromo-2-methylpropyl 2-(6-methoxynaphthalen-2-yl)propanoate (derivative of Naproxen) R3, in solvents of increasing polarity.

Comp.		Y		CCl_4		$CHCl_3$		CH_3CN	
		ν_{CO}	P	$2\nu_{CO}$	P	ν_{CO}	P	ν_{CO}	P
R_1	OMe	1743	90	3469	84	1725	18	1738	76
		1759	10	3492	16	1738	72	1748	24
	H	1743	70	3471	77	1729	41	1738	73
		1754	30	3493	23	1741	59	1748	27
	Cl	1747	100	3474	100	1729	36	1737	55
		-	-	-	-	1741	64	1746	45
	NO_2	1748	84	3474	69	1734	44	1742	92
		1761	16	3489	31	1744	56	1757	8
R_2		1731	10	3450	22	1724	33	1725	87
		1743	90	3470	78	1736	67	1738	13
R_3		1734	21	3451	17	1720	18	1728	18
		1744	79	3468	83	1734	82	1738	82

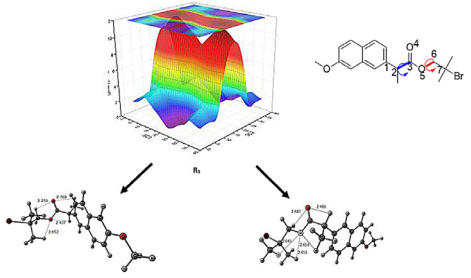

Each compound was purified by column chromatography on silica gel using hexane/ethyl acetate as the eluent. The structures of all the compounds were determined by ^1H NMR, ^{13}C NMR, GC-MS (ESI), elemental analysis, and IR (Supporting Information).

2.2. Infrared spectroscopy

Infrared spectra for the solutions were obtained on a FT-IR Michelson Bomem™ MB100 spectrometer with 1.0 cm^{-1} resolution, in the 4000–600 cm^{-1} range. The solutions were properly prepared at a concentration of 0.02 mol•L^{-1} in CCl_4, CH_3Cl, and CH_3CN. For measurement of the carbonyl stretching band, we used a NaCl cell with a 0.5-mm optical path. The determinations in the first harmonic region were obtained in a quartz cell with a 1.0-cm optical path, in CCl_4. The GRAMS/4.04 program was used to analyze the bands [19]. The population of conformers was estimated from the maximum of each component of the resolved carbonyl doublet, and was expressed as a percentage of the absorbance, assuming equimolar absorptivity coefficients for the referred conformers.

2.3. Computational methods

Calculations were performed using the Gaussian 09 program [20] in Linux environment with 64-bits Ubuntu with three servers, two of which contained 16 processors in two Intel® Xeon eight-core E5-26770 sockets of 2.6 GHz, 128 GB RAM, and a 9-TB disk, while the other contained two Intel® Xeon® six-core 5560 sockets, 12 processors with 96 GB of RAM, and a 3-TB disk.

Representations of the molecular structures were plotted in the Gaussview [21] and ChemCraft [22] visualization programs.

Density functional theory (DFT) was applied to investigate the conformational changes with the functional hybrid B3LYP [23–25] and standard 6-311+G (2df,2p) basis set. The orbital interactions were calculated in NBO 3.1 [26].

3. Results and discussion

3.1. Infrared spectroscopy analysis

Table 1 shows the frequency and intensity of the carbonyl stretching bands of compounds **R1–R3**, which were analytically

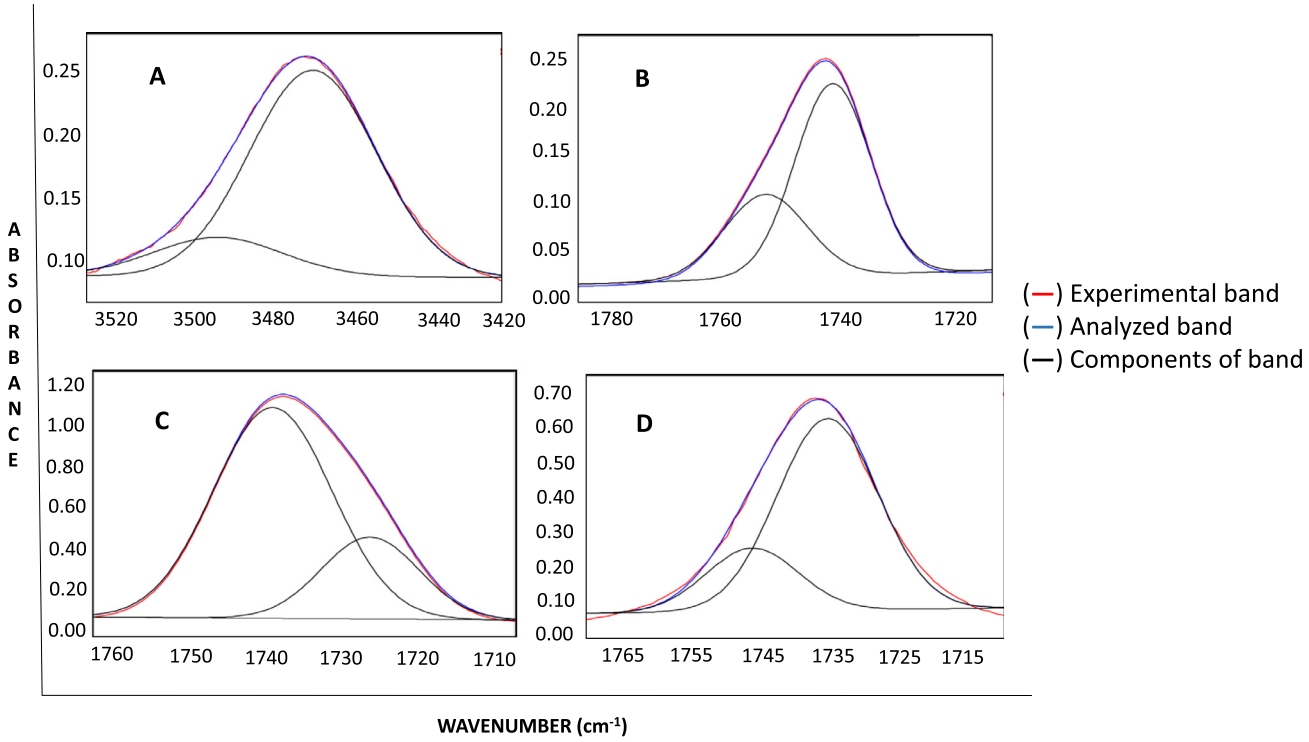

Fig. 1. IR analytically resolved carbonyl stretching bands of 2-bromo-2-methylpropyl 2-(4-isobutylphenyl)propanoate **R2**, ibuprofen derivative, in carbon tetrachloride [(**A**)first overtone and (**C**)fundamental)], chloroform (**C**) and acetonitrile (**D**).

solved for the $\nu_{C=O}$ fundamental transition, in solvents with increasing polarity (CCl_4, $\varepsilon = 2.22$; $CHCl_3$, $\varepsilon = 4.7$; CH_3CN, $\varepsilon = 35.68$) and in the first harmonic region recorded in CCl_4.

For compounds **R1–R3**, analysis shows that these bands exhibit the same behavior in both the fundamental state and the first harmonic region in CCl_4, (Fig. 1, for **R2**). Two bands were observed in the carbonyl stretching region ($\nu_{C=O}$) and the first harmonic region, corresponding to twice the frequency observed in the fundamental region minus an anharmonicity value. All the compounds except **R1** (Y = Cl), which has one single carbonyl stretching band, exhibited identical behavior.

The lowest frequency band for compound **R1** in CCl_4 ($\varepsilon = 2.22$) corresponds to the highest population. In contrast, for compounds **R2** and **R3**, the highest frequency band corresponded to the highest population. The opposite behavior was observed in $CHCl_3$ ($\varepsilon = 4.7$) for all the investigated compounds except **R3**, for which the band population followed the same trend as observed in CCl_4.

The same behavior was observed in the most polar solvent (CH_3CN ($\varepsilon = 35.68$)) as well as in the least polar solvent (CCl_4) for compounds **R1** and **R3** (naproxen derivatives). However, compound **R2** (an ibuprofen derivative) exhibited the opposite behavior, where the lowest frequency conformer displayed the highest population.

Another important observation from Table 1 is that increasing the solvent polarity modified the behavior of compounds **R1–R3** and caused a decrease in the carbonyl stretching frequency for all bands. These results are consistent with the fact that the C=O bond order decreases in more polar solvents, which causes a decrease in the $\nu_{C=O}$ value.

3.2. Conformational search using theoretical calculations

A conformational search was performed for compounds **R1-R3** to determine the main (most stable) conformation. To ensure that no degrees of freedom in the studied molecules were neglected,

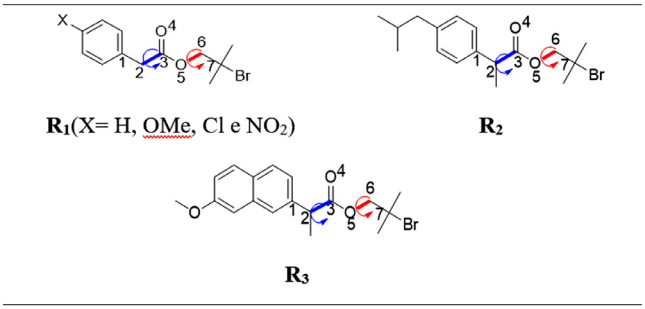

Fig. 2. Selected dihedral angles in conformational search, **SC1**=C1-C2-C3-O4 and **SC2**=C3-O5-C6-C7 in relation to carbonyl group, for the **R1–R3** compounds.

we performed a relaxed double scan, considering two dihedral angles to have the greatest influence on the conformations of this series of compounds in relation to the carbonyl group. The Gaussian 09 [18] program was used to construct the surface graphs, which display the conformer energy as a function of the rotational movement applied to the two dihedral angles (Fig. 2).

The selected angles were rotated at intervals from 10 to 360° (dihedral angles SC1 = C1-C2-C3-O4 and SC2 = C3-O5-C6-C7) using density functional theory (DFT) with the B3LYP hybrid functional [19–22]. The description of the atomic centers (H, C, O, N, and Br) utilized the standard 6-31G(d,p) data set (Fig. 3).

3.3. Theoretical calculations: conformational equilibrium

After identifying the minimum on the potential surface graphs, the corresponding conformations were optimized at the DFT-B3LYP/6-311+G(2df,2p) and DFT-M062X/6-311+G(2df,2p) levels of theory to identify all the significant differences between the two methods. The dihedral angles were assigned in relation to the α dihedral angle (Fig. 4).

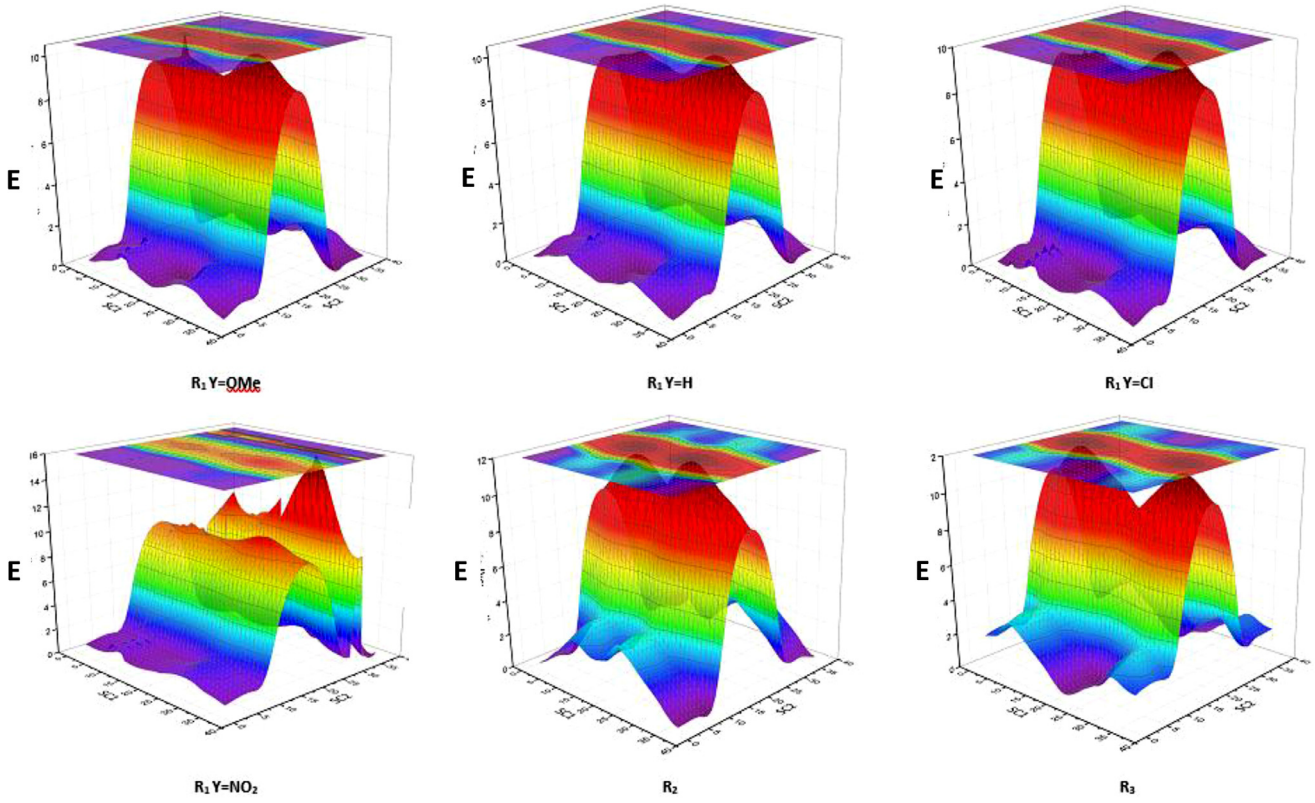

Fig. 3. Energy surface graphics as a function of the rotation of SC1=C1-C2-C3-O4 and SC2=C3-O5-C6-C7 dihedral angles, optimized at AM1 semi-empirical level, for the **R1–R3** compounds.

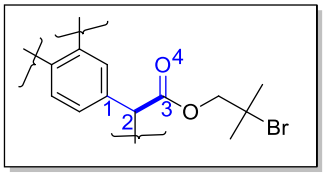

Fig. 4. The α=C1-C2-C3-O4 dihedral angle.

A search using two density functionals is necessary to determine the method with the best correlation to the experimental data. The DFT-BYLYP level was more precise for determining the populations compared to the DFT-M062X level, where the latter showed the conversion of one of the local minima into a global minimum in the identified conformations.

The results obtained using the DFT-B3LYP/6-311+G(2df,2p) calculations for the global minimum in relation to α = C1-C2-C3-O4 indicated the stability of the following conformations: compound **R1** (Y = NO_2) preferentially adopts a gauche conformation (g); when there is a small variation in the dihedral angle for compounds **R1** (Y = H, OMe, and Cl) and **R2–R3**, an anti-clinal (ac) and quasi-gauche (q-g) geometry is preferentially formed (Table 2). The local minima (highest energy conformers) for **R1** (Y = H, OMe, Cl, and NO_2) were calculated, and the a and b dihedral angles were found to differ significantly for higher energy conformers in relation to the global minimum (lowest energy conformers).

However, for compounds **R2** and **R3**, the lowest and highest energy conformations were not significantly different, where both adopted an anti-clinal (ac) conformation.

Compound **R1** (Y = OMe) presents two stable conformations: a low-energy anti-clinal (ac_1) conformation with 73% population, 0 kcal.mol^{-1} energy, and high polarity (4.51 D), and a gauche (g_2) conformation with 0.60 kcal.mol^{-1} energy and low polarity (2.56 D). The $\nu_{C=O}$ values for the two conformers differ by 8 cm^{-1} (Fig. 5).

A search using two density functionals is necessary to determine the method with the best correlation to the experimental data. The DFT-BYLYP level provided a more precise approximation of the populations of the conformers than the DFT-M062X level, where the latter showed the conversion of one of the local minima into a global minimum in the identified conformations.

The DFT-B3LYP/6-311+G(2df,2p) calculations of the global minimum in relation to α = C1-C2-C3-O4 indicated the stability of the following conformations: the gauche conformation (g) was preferential for compound **R1** (Y = NO_2) and was preferred for compounds **R1** (Y = H, OMe, and Cl) when there was a small variation in the dihedral angle; **R2** and **R3** preferentially adopted an anti-clinal (ac) and quasi-gauche (q-g) geometry, respectively (Table 2). The local minima (highest energy conformers) for **R1** (Y = H, OMe, Cl, and NO_2) were calculated and the a and b dihedral angles in the global minimum (lowest energy conformers) were significantly different from those in higher energy conformers. However, compounds **R2** and **R3** did not display any significant variation between the lowest and highest energy conformations, where both adopted an anti-clinal (ac) conformation.

Compound **R1** (Y = OMe) presents two stable conformations: a low-energy anti-clinal (ac_1) conformation with 73% population, 0 kcal.mol^{-1} energy, and high polarity (4.51 D), and a gauche (g_2) conformation with 0.60 kcal.mol^{-1} energy and low polarity (2.56 D). The $\nu_{C=O}$ values for the two conformers differ by 8 cm^{-1} (Fig. 5).

Compound **R1** (Y = H) preferentially adopts two conformations: a low-energy anti-clinal (ac_1) conformation with 75% population, 0 kcal.mol^{-1} energy, and high polarity (3.30 D) and a less stable gauche (g_2) conformation with 0.65 kcal.mol^{-1} energy and low po-

Table 2
Relative free energy (kcal mol^{-1}), relative population (%), calculated stretching band ($\nu_{C=O,}$ cm^{-1}), dipole moment (μ/D) and selected dihedral angles (deg) for the different conformers of 2-bromo-2-methylpropyl-2-aryl-acetate-*para*-substituted R1 (X = H, OMe, Cl and NO_2), 2-bromo-2-methylpropyl-2-(4-isobutylphenyl)propanoate (derivative of Ibuprofen) R2 and-2-bromo-2-methylpropyl 2-(6-methoxynaphthalen-2-yl)propanoate (derivative of Naproxen) R3, at the DFT/6-311+G (2df.2p) level of theory.

								Dihedral angles /^{o} [c]								
Comp.	Y	Conf.	[a]E	[b]P (%)	[d]$\nu_{C=O}$	μ/D	α	β	γ	δ	ε	ϕ	ω	φ	α'	β'
R_1	**OMe**	$ac_{(1)}$	0	73	1790	4.51	96.67	-82.29	178.50	-112.65	-0.47	61.07	67.32	-176.64	-	-
		$g_{(1)}$	0.60	27	1798	2.56	-35.57	146.50	175.37	114.72	-2.57	-66.60	61.87	177.56	-	-
	H	$ac_{(1)}$	0	75	1790	3.30	-95.26	83.73	-178.70	112.52	0.29	61.18	-67.25	177.82	-	-
		$g_{(1)}$	0.65	25	1799	2.89	-37.05	145.01	175.13	116.42	-2.82	61.59	-66.89	177.25	-	-
	Cl	$ac_{(1)}$	0	100	1788	3.06	3.06	94.01	177.47	-175.61	-1.27	-63.45	64.88	-179.25	-	-
	NO_2	$g_{(1)}$	*0*	66	1790	6.97	-88.09	90.06	176.02	178.03	2.74	54.0	179.41	-64.61	-	-
		$c_{(1)}$	0.38	34	1800	6.61	-23.42	15.01	179.22	-144.0	0.64	57.0	61.39	177.11	-	-
R_2		$ac_{(2)}$	1.23	11	1782	3.90	-107.62	73.32	-178.59	175.05	1.09	-64.96	63.46	179.23	124.02	-56.25
		$ac_{(1)}$	0	89	1788	3.56	-94.0	-84.94	177.63	-116.04	-1.32	67.41	-60.91	-176.64	-30.72	150.32
R_3		$ac_{(2)}$	1.29	10	1783	3.73	-97.32	81.99	-178.12	-175.90	1.20	64.18	-64.35	179.21	134.54	-46.14
		$ac_{(1)}$	0	90	1787	4.90	93.52	-85.54	-174.76	-116.04	-0.54	67.28	-61.20	-176.86	-31.24	-144.68

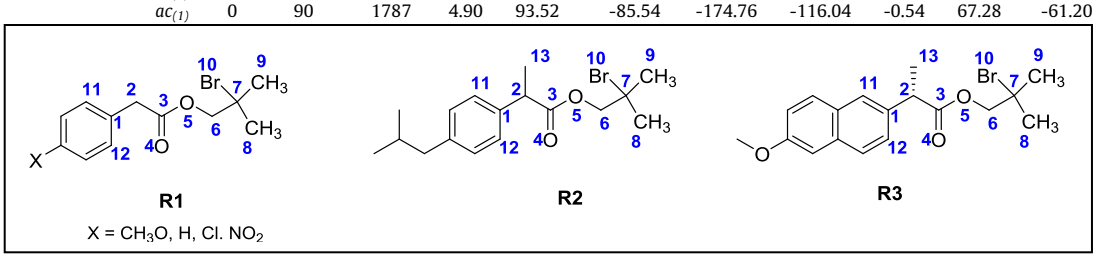

[a] The relative free Gibbs energy (relative electronic energy plus ZPE correction).
[b] The relative population is reported as a percentage. [e]α=C(1)-C(2)-C(3)-O(4); β=C(1)-C(2)-C(3)-O(5); γ=C(2)-C(3)-O(5)-C(6); δ=C(3)-O(5)-C(6)-C(7); ε=O(4)-C(3)-O(5)-C(6);ϕ=O(5)-C(6)-C(7)-C(8); ω=O(5)-C(6)-C(7)-C(9); φ=O(5)-C(6)-C(7)-Br(10); α'=C(13)-C(2)-C(3)-O(4); β'=C(13)-C(2)-C(3)-O(5).

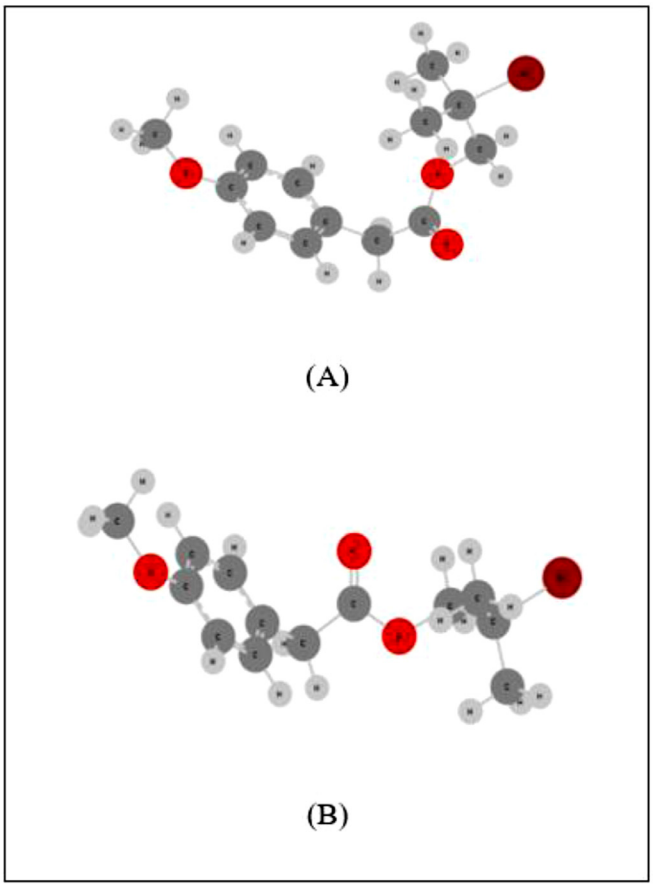

Fig. 5. Structural representations calculated at the DFT / B3LYP / 6-311 + G (2df, 2p) level of theory for the lowest energy (A) and highest energy (B) conformers of 2-bromo-2-methylpropyl 2-(4'-methoxyphenylacetate) [**R_1** (Y= OMe)].

larity (2.89 D). The difference in the calculated ν_{CO} values for the two equilibrium geometries was 9 cm^{-1}. A single stable anti-clinal (ac_1) conformation was found for compound **R1** (Y = Cl), with a dipole moment of 3.06 D and a carbonyl stretching frequency of 1788 cm^{-1}. Two stable conformations were identified for compound **R1** (Y = NO_2): a low-energy gauche (g_1) conformation with 66% population, 0 kcal.mol^{-1} energy, and high polarity (6.97 D), and a less stable conformation cis (c_2) with 0.38 kcal.mol^{-1} energy and low polarity (6.61 D). The difference in the calculated $\nu_{C=O}$ values for the two conformations was 10 cm^{-1}.

Compound **R2** (ibuprofen derivative) displayed two stable conformations: a low-energy gauche (ac_1) conformation with 89% population, 0 kcal.mol^{-1} energy, and low polarity (3.56 D) and a less stable anti-clinal (ac_2) conformation with 1.23 kcal.mol^{-1} energy and high polarity (3.90 D). The difference in the calculated $\nu_{C=O}$ values for the two conformations was 6 cm^{-1}. Two stable conformations were also observed for compound **R3** (a naproxen derivative): a low-energy anti-clinal (ac_1) conformation with 90% population, 0 kcal.mol^{-1} energy, and low polarity (3.73 D) and a less stable anti-clinal (ac_2) conformer with 1.29 kcal.mol^{-1} energy and high polarity (4.90 D). The corresponding $\nu_{C=O}$ values for the two structures differ by 5 cm^{-1}.

No significant changes were found in the other dihedral angles in all stable conformers of compounds **R1–R3**. The calculated carbonyl stretching frequencies for all the studied compounds and the relative populations of the conformers were consistent with the experimentally obtained values from the IR spectra recorded in CCl_4. Thus, it is inferred that the two bands found in the IR spectra must correspond to the two computationally found conformations.

3.4. Calculations with solvent effects

Theoretical calculations conducted for the gas phase indicate that compounds **R1–R3** adopt the ac conformation, except for **R1** with Y = Cl for which the minimum energy corresponds to the g conformation.

Table 3
Relative free energy (kcal mol^{-1}), relative population (%), calculated stretching band ($\nu_{C=O}$/cm^{-1}), dipole moment (μ/D), and selected dihedral angles (deg) for the different conformers of 2-bromo-2-methylpropyl-2-aryl-acetate-*para*-substituted R1 (X = H, OMe, Cl and NO_2), 2-bromo-2-methylpropyl 2-(4-isobutylphenyl)propanoate (derivative of Ibuprofen) R2 and 2-bromo-2-methylpropyl 2-(6-methoxynaphthalen-2-yl)propanoate (derivative of Naproxen) R3, at the DFT-M062X/6-311+G(2df,2p) level of theory and IEF PCM method (polarizable continuum model).

								Dihedral angles /° [c]								
Comp	Y	Conf.	[a]E	[b]P (%)	[d]$\nu_{C=O}$	μ/D	α	β	γ	δ	ε	ϕ	ω	φ	α'	β'
R_1	**OMe**	$ac_{(1)}$	0	100	1855	4.35	96.80	79.63	-168.89	-100.71	7.57	63.45	62.95	-179.50	-	-
	H	$ac_{(1)}$	0	98	1856	2.81	-98.13	78.53	169.29	100.30	7.38	62.41	-64.30	178.97		
		$g_{(1)}$	2.43	2	1857	2.81	-39.86	141.76	177.05	100.94	1.33	61.63	-65.15	178.00		
	Cl	$ac_{(1)}$	0	100	1857	2.99	103.66	-74.20	174.75	-173.23	-3.51	63.21	-63.37	179.90		
	NO_2	$g_{(1)}$	0	75	1860	6.62	-101.23	76.66	-172.32	172.73	5.61	55.84	-179.26	-62.66		
		$c_{(1)}$	0.67	24	1862	5.87	-16.90	164.69	177.86	-100.88	-0.56	63.52	-63.18	-179.83		
R_2		$ac_{(1)}$	2.55	1	1849	3.64	-116.34	63.76	-177.43	165.45	2.70	61.20	-65.07	178.01	117.33	-62.52
		$ac_{(2)}$	0	99	1852	3.92	95.38	-81.27	168.47	-102.01	-8.20	64.85	-61.35	-178.08	154.77	-28.62
R_3		$ac_{(2)}$	2.48	2	1852	3.84	-116.21	63.69	-177.30	171.53	2.59	61.99	-64.45	178.78	177.42	-62.67
		$ac_{(1)}$	0	92	1853	4.52	95.74	-81.00	168.98	-99.41	-7.78	66.45	-59.93	-178.56	154.73	-28.52

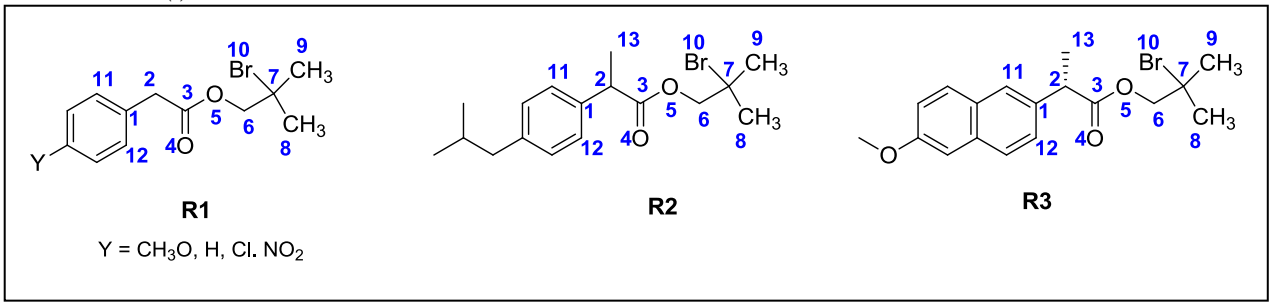

[a] The relative free Gibbs energy (relative electronic energy plus ZPE correction).
[b] The relative population is reported as a percentage.[c] α=C(1)-C(2)-C(3)-O(4);β=C(1)-C(2)-C(3)-O(5);γ=C(2)-C(3)-O(5)-C(6);δ=C(3)-O(5)-C(6)-C(7);ε=O(4)-C(3)-O(5)-C(6);ϕ=O(5)-C(6)-C(7)-C(8);ω=O(5)-C(6)-C(7)-C(9);φ=O(5)-C(6)-C(7)-S(10); Ψ= C(7)-S(10)-N(13)-O(14); α'=C(15)-C(2)-C(3)-O(4); β'=C(15)-C(2)-C(3)-O(5).

The solvent effects were incorporated using the IEF PCM method (polarizable continuum model) [27]. The starting geometries were obtained from the gas-state calculations and optimized; the carbonyl stretching frequencies and relative conformer populations are shown in Table 3. Overall, the solvent exerted a considerable effect on the calculated conformations.

IEF PCM did not exactly reproduce the experimentally observed behavior, but indicated a clear trend in polar solvents, where there was a population inversion for compound **R1** compared to the experimental data. In the ac conformers, solvation of the carbonyl region is less hindered, which may justify the observed results. This trend was not pronounced for **R2** and **R3**, which is attributed to the presence of the methyl group in the α-position, which reduces the possibility of forming intramolecular hydrogen bonds with the carbonyl group and makes solvation difficult. Solvation calculations using IEF PCM failed to accurately describe the experimental data, but the trends were very similar to the experimental results. We believe that the use of other solvation calculation methods such as PCM-SMD or even IEF PCM, which specifies the solvent molecule in the starting geometry, may lead to more satisfactory results.

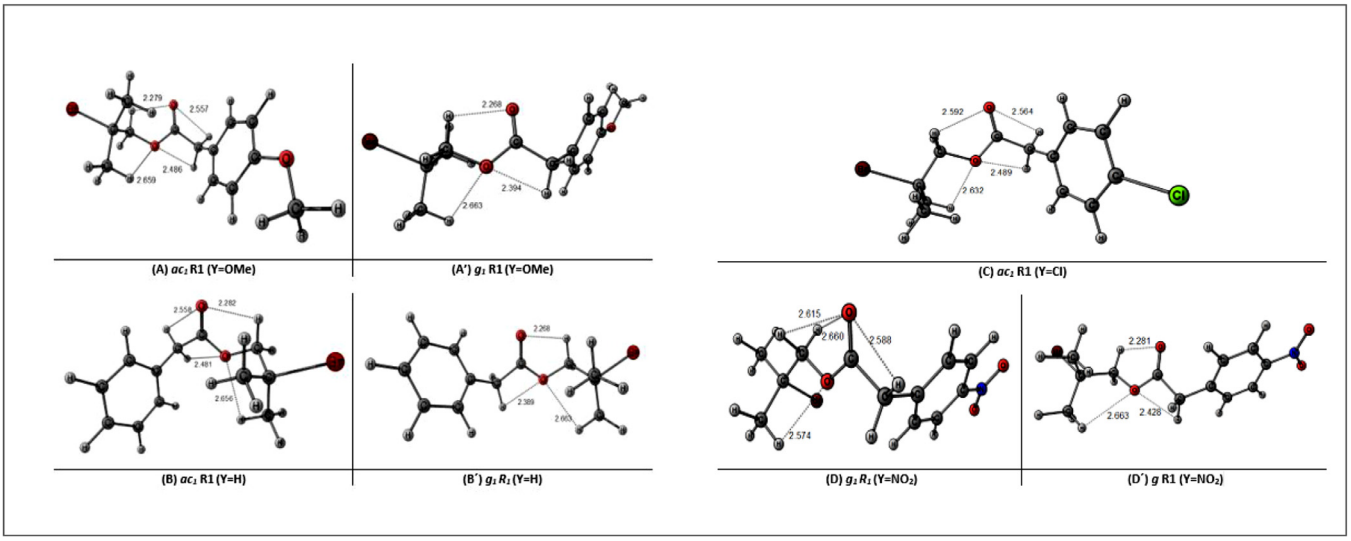

Fig. 6. Molecular graphs for the *ac* conformers of the compounds **R1**(Y= H, OMe, Cl and NO_2) showing electrostatic and charge transfer (intramolecular hydrogen bonds) interactions between the negative oxygen atoms in the carbonyl and the ester groups and the adjacent hydrogen atoms.

Table 4
Energy of orbital interactions calculated by the Natural Bond Orbital method (kcal.mol^{-1}) for the 2-bromo-2-methylpropyl-2-aryl-acetate-*para*-substituted **R1** (X = H. OMe. Cl and NO_2).

R_1 Y=OMe			R_1 Y=H			R_1 Y=Cl		R_1 Y = NO_2		
Orbital Interaction	$ac_{(1)}$	$g_{(1)}$	Orbital Interaction	$ac_{(1)}$	$g_{(1)}$	Orbital Interaction	$ac_{(1)}$	Orbital Interaction	$g_{(1)}$	$c_{(1)}$
$\sigma_{C(2)-C(3)}\rightarrow\sigma^*_{C(3)-C(4)}$	3.55	3.24	$\pi_{C(3)-C(4)}\rightarrow\sigma^*_{C(12)-H(14)}$	1.92	2.28	$\sigma_{C(3)-C(4)}\rightarrow\sigma^*_{C(2)-C(3)}$	3.46	$\pi_{C(2)-C(4)}\rightarrow\sigma^*_{C(11)-C(14)}$	3.01	3.36
$\pi_{C(2)-C(3)}\rightarrow\sigma^*_{C(14)-O(15)}$	1.09	-	$\pi_{C(3)-C(4)}\rightarrow\sigma^*_{C(12)-H(14)}$	3.32	-	$\sigma_{C(3)-C(4)}\rightarrow\sigma^*_{C(5)-H(10)}$	2.24	$\pi_{C(2)-C(4)}\rightarrow\pi^*_{C(11)-C(14)}$	1.14	-
$\sigma_{C(3)-C(11)}\rightarrow\sigma^*_{C(14)-O(15)}$	1.17	-	$\pi_{C(3)-C(4)}\rightarrow\pi^*_{C(15)-O(16)}$	0.99	-	$\sigma_{C(3)-C(4)}\rightarrow\sigma^*_{C(1)-C(2)}$	2.42	$\sigma_{C(3)-C(11)}\rightarrow\pi^*_{C(14)-O(15)}$	3.47	1.91
$\sigma_{C(3)-C(11)}\rightarrow\pi^*_{C(14)-O(15)}$	3.25	4.27	$\sigma_{C(3)-C(12)}\rightarrow\sigma^*_{C(15)-O(17)}$	-	1.73	$\sigma_{C(3)-C(11)}\rightarrow\sigma^*_{C(4)-C(5)}$	2.45	$\sigma_{C(3)-C(11)}\rightarrow\sigma^*_{C(14)-O(15)}$	4.46	-
$\pi_{C(4)-C(5)}\rightarrow\pi^*_{C(2)-C(3)}$	18.09	17.69	$\sigma_{C(3)-C(12)}\rightarrow\sigma^*_{C(15)-O(16)}$	1.11	-	$\sigma_{C(3)-C(11)}\rightarrow\pi^*_{C(14)-O(15)}$	3.33	$\sigma_{C(4)-H(9)}\rightarrow\sigma^*_{C(5)-C(6)}$	3.59	-
$\sigma_{C(11)-H(12)}\rightarrow\sigma^*_{C(2)-C(3)}$	2.68	4.09	$\sigma_{C(3)-C(12)}\rightarrow\pi^*_{C(15)-O(16)}$	3.26	-	$\sigma_{C(5)-C(6)}\rightarrow\sigma^*_{C(1)-C(6)}$	3.68	$\pi_{C(5)-C(6)}\rightarrow\pi^*_{C(1)-C(2)}$	20.86	20.35
$\sigma_{C(11)-H(12)}\rightarrow\sigma^*_{C(14)-O(16)}$	3.91	-	$\pi_{C(5)-C(6)}\rightarrow\pi^*_{C(1)-C(2)}$	20.34	19.90	$\sigma_{C(5)-C(6)}\rightarrow\sigma^*_{C(4)-C(5)}$	3.06	$\sigma_{C(11)-H(12)}\rightarrow\sigma^*_{C(2)-C(3)}$	-	3.53
$\sigma_{C(11)-H(13)}\rightarrow\sigma^*_{C(3)-C(4)}$	3.97	2.40	$\pi_{C(5)-C(6)}\rightarrow\pi^*_{C(3)-C(4)}$	20.12	20.03	$\sigma_{C(5)-C(6)}\rightarrow\sigma^*_{C(4)-H(9)}$	2.13	$\sigma_{C(11)-H(12)}\rightarrow\sigma^*_{C(14)-O(15)}$	-	2.75
$\sigma_{C(11)-H(13)}\rightarrow\sigma^*_{C(14)-O(15)}$	-	1.56	$\sigma_{C(5)-H(10)}\rightarrow\sigma^*_{C(15)-O(16)}$	3.82	-	$\sigma_{C(11)-C(14)}\rightarrow\sigma^*_{O(16)-C(18)}$	4.07	$\sigma_{C(11)-H(12)}\rightarrow\sigma^*_{C(3)-C(4)}$	3.47	2.38
$\sigma_{C(11)-H(13)}\rightarrow\sigma^*_{C(14)-O(15)}$	3.45	4.27	$\sigma_{C(6)-H(11)}\rightarrow\sigma^*_{C(4)-C(5)}$	3.79	-	$\sigma_{C(21)-Br(14)}\rightarrow\sigma^*_{O(16)-C(18)}$	4.84	$\sigma_{C(11)-H(12)}\rightarrow\pi^*_{C(3)-C(4)}$	1.05	-
$\sigma_{C(11)-H(13)}\rightarrow\pi^*_{C(14)-O(15)}$	2.76	6.80	$\sigma_{C(12)-H(13)}\rightarrow\sigma^*_{C(15)-O(16)}$	3.52	4.28	$\sigma_{C(22)-H(23)}\rightarrow\sigma^*_{C(18)-C(21)}$	4.02	$\sigma_{C(11)-H(12)}\rightarrow\sigma^*_{C(14)-O(15)}$	3.99	6.27
$\sigma_{C(11)-C(14)}\rightarrow\pi^*_{C(2)-C(3)}$	2.39	1.92	$\sigma_{C(12)-H(13)}\rightarrow\pi^*_{C(15)-O(16)}$	2.57	1.46	$\sigma_{C(22)-H(25)}\rightarrow\sigma^*_{C(21)-C(26)}$	4.11	$\sigma_{C(11)-H(12)}\rightarrow\pi^*_{C(14)-O(15)}$	1.36	-
$\sigma_{C(11)-C(13)}\rightarrow\sigma^*_{O(16)-C(17)}$	4.16	3.97	$\sigma_{C(12)-H(14)}\rightarrow\sigma^*_{C(15)-O(16)}$	2.55	2.39	$\sigma_{C(22)-H(25)}\rightarrow\sigma^*_{C(21)-C(26)}$	4.03	$\sigma_{C(11)-H(13)}\rightarrow\sigma^*_{C(2)-C(3)}$	3.33	-
$\sigma_{C(17)-H(19)}\rightarrow\sigma^*_{C(20)-C(25)}$	3.90	3.85	$\sigma_{C(12)-H(14)}\rightarrow\pi^*_{C(3)-O(4)}$	2.23	2.52	$\sigma_{C(26)-H(28)}\rightarrow\sigma^*_{C(21)-C(22)}$	4.09	$\sigma_{C(11)-H(13)}\rightarrow\pi^*_{C(14)-O(15)}$	1.57	-
$\sigma_{C(21)-H(22)}\rightarrow\sigma^*_{C(20)-C(25)}$	4.06	-	$\sigma_{C(12)-H(14)}\rightarrow\sigma^*_{C(15)-O(16)}$	-	6.67	$\eta_{2\ O(15)}\rightarrow\sigma^*_{C(11)-C(14)}$	18.87	$\sigma_{C(11)-H(13)}\rightarrow\sigma^*_{C(4)-O(16)}$	3.25	-
$\eta_{1\ O(15)}\rightarrow\sigma^*_{C(11)-C(14)}$	2.36	2.27	$\sigma_{C(12)-H(14)}\rightarrow\sigma^*_{C(15)-O(17)}$	3.83	-	$\eta_{2\ O(15)}\rightarrow\sigma^*_{C(11)-O(16)}$	35.12	$\sigma_{C(11)-C(14)}\rightarrow\pi^*_{C(3)-C(4)}$	2.74	1.04
$\eta_{2\ O(15)}\rightarrow\sigma^*_{C(11)-C(14)}$	18.65	19.45	$\sigma_{C(12)-C(15)}\rightarrow\sigma^*_{C(3)-C(4)}$	1.03	-	$\eta_{1\ O(16)}\rightarrow\sigma^*_{C(14)-O(15)}$	7.81	$\sigma_{C(11)-C(14)}\rightarrow\sigma^*_{C(3)-C(11)}$	1.03	
$\eta_{2\ O(15)}\rightarrow\sigma^*_{C(14)-O(16)}$	35.44	35.65	$\sigma_{C(12)-C(15)}\rightarrow\sigma^*_{C(3)-C(12)}$	1.06	-	$\eta_{2\ O(16)}\rightarrow\sigma^*_{C(14)-O(15)}$	48.35	$\sigma_{C(11)-C(14)}\rightarrow\sigma^*_{C(14)-O(15)}$	1.15	
$\eta_{1\ O(16)}\rightarrow\sigma^*_{C(14)-O(15)}$	8.34	8.11	$\eta_{2\ O(16)}\rightarrow\sigma^*_{C(12)-C(15)}$	18.77	19.56			$\sigma_{C(11)-C(14)}\rightarrow\sigma^*_{O(16)-C(20)}$	4.15	4.01
$\eta_{1\ O(16)}\rightarrow\sigma^*_{C(17)-H(18)}$	2.64	1.06	$\eta_{2\ O(16)}\rightarrow\sigma^*_{C(15)-O(17)}$	35.33	35.58			$\sigma_{O(16)-C(20)}\rightarrow\sigma^*_{C(11)-C(14)}$	2.33	2.20
$\eta_{1\ O(16)}\rightarrow\sigma^*_{C(17)-H(19)}$	1.11	2.64	$\eta_{1\ O(16)}\rightarrow\sigma^*_{C(15)-O(17)}$	8.40	8.13			$\sigma_{C(20)-H(21)}\rightarrow\sigma^*_{C(23)-Br(32)}$	7.04	2.60
$\eta_{2\ O(16)}\rightarrow\pi^*_{C(14)-O(15)}$	47.33	44.75	$\eta_{2\ O(16)}\rightarrow\sigma^*_{C(15)-O(16)}$	47.77	44.58			$\sigma_{C(20)-H(22)}\rightarrow\sigma^*_{C(23)-C(24)}$	4.00	3.83
			$\eta_{12O(16)}\rightarrow\sigma^*_{C(18)-c(21)}$	3.65	3.43			$\sigma_{C(23)-C(28)}\rightarrow\sigma^*_{O(16)-C(20)}$	2.97	-
								$\sigma_{C(28)-H(31)}\rightarrow\sigma^*_{C(23)-Br(32)}$	6.84	5.02
								$\eta_{1\ O(15)}\rightarrow\sigma^*_{C(11)-C(14)}$	2.32	7.05
								$\eta_{2\ O(15)}\rightarrow\sigma^*_{C(11)-C(14)}$	19.23	20.40
								$\eta_{2\ O(15)}\rightarrow\sigma^*_{C(14)-O(16)}$	34.96	35.18
								$\eta_{1\ O(16)}\rightarrow\sigma^*_{C(14)-O(15)}$	7.93	8.40
								$\eta_{1\ O(16)}\rightarrow\pi^*_{C(14)-O(15)}$	49.75	46.63
								$\eta_{2\ O(16)}\rightarrow\sigma^*_{C(20)-H(21)}$	4.75	3.18
								$\eta_{2\ O(16)}\rightarrow\sigma^*_{C(20)-H(22)}$	4.74	3.46
Σ (kcal.mol^{-1})	136.59	113.93	Σ (kcal.mol^{-1})	197.71	172.54					
.54	Σ (kcal.mol^{-1})	158.08	Σ (kcal.mol^{-1})	210.48	186.55					

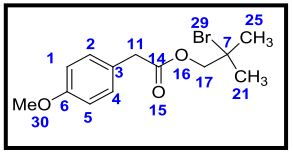

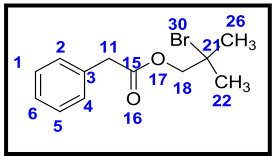

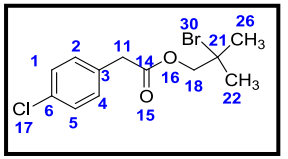

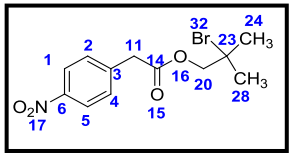

Table 5
Energy of electronic interactions calculated by the Natural Bond Orbital method (kcal.mol-1), for the 2-bromo-2-methylpropyl 2-(4-isobutylphenyl)propanoate (derivative of Ibuprofen) **R2** and 2-bromo-2-methylpropyl 2-(6-methoxynaphthalen-2-yl)propanoate (derivative of Naproxen) **R3.**

R2 Ibuprofen			R3 Naproxen		
Orbital interaction	$ac_{(2)}$	$ac_{(1)}$	Orbital interaction	$ac_{(2)}$	$ac_{(1)}$
$\sigma_{C(1)-C(6)} \rightarrow \sigma^*_{C(1)-C(2)}$	-	3.22	$\pi_{C(9)-C(14)} \rightarrow \pi^*_{C(3)-C(4)}$	15.76	15.88
$\pi_{C(2)-C(3)} \rightarrow \sigma^*_{C(11)-C(13)}$	-	2.82	$\pi_{C(9)-C(14)} \rightarrow \pi^*_{C(10)-C(13)}$	16.92	17.25
$\pi_{C(2)-C(3)} \rightarrow \sigma^*_{C(11)-C(16)}$	3.53	2.74	$\pi_{C(10)-C(13)} \rightarrow \pi^*_{C(9)-C(14)}$	17.31	16.81
$\sigma_{C(3)-C(4)} \rightarrow \sigma^*_{C(2)-H(8)}$	2.66	2.75	$\sigma_{C(14)-H(16)} \rightarrow \sigma^*_{C(3)-C(9)}$	4.29	4.37
$\sigma_{C(3)-C(11)} \rightarrow \sigma^*_{C(4)-C(5)}$	2.30	2.37	$\sigma_{C(17)-H(18)} \rightarrow \sigma^*_{C(19)-H(21)}$	-	1.01
$\sigma_{C(3)-C(11)} \rightarrow \pi^*_{C(13)-O(14)}$	2.91	3.10	$\sigma_{C(14)-H(16)} \rightarrow \sigma^*_{C(19)-H(21)}$	2.85	2.59
$\sigma_{C(3)-C(11)} \rightarrow \sigma^*_{C(16)-H(17)}$	-	1.31	$\sigma_{C(17)-H(18)} \rightarrow \sigma^*_{C(23)-O(25)}$	3.90	3.75
$\sigma_{C(4)-H(9)} \rightarrow \sigma^*_{C(2)-C(3)}$	4.43	4.57	$\sigma_{C(17)-H(18)} \rightarrow \pi^*_{C(23)-O(25)}$	1.70	2.54
$\sigma_{C(4)-H(9)} \rightarrow \sigma^*_{C(5)-C(6)}$	-	3.92	$\sigma_{C(17)-C(19)} \rightarrow \sigma^*_{C(10)-C(13)}$	-	2.12
$\sigma_{C(4)-H(12)} \rightarrow \sigma^*_{C(3)-C(4)}$	4.08	4.60	$\sigma_{C(17)-C(19)} \rightarrow \sigma^*_{C(23)-O(24)}$	4.62	2.53
$\sigma_{C(11)-H(12)} \rightarrow \sigma^*_{C(13)-O(14)}$	4.85	3.71	$\sigma_{C(17)-C(23)} \rightarrow \pi^*_{C(10)-C(13)}$	2.36	1.95
$\sigma_{C(11)-H(12)} \rightarrow \pi^*_{C(13)-O(14)}$	-	2.68	$\sigma_{C(17)-C(23)} \rightarrow \sigma^*_{O(24)-C(31)}$	2.30	4.11
$\sigma_{C(11)-H(12)} \rightarrow \sigma^*_{C(16)-H(18)}$	2.95	2.59	$\sigma_{C(17)-H(22)} \rightarrow \sigma^*_{C(17)-C(23)}$	3.18	2.94
$\sigma_{C(11)-H(13)} \rightarrow \sigma^*_{O(15)-C(33)}$	3.95	4.12	$\sigma_{O(24)-C(31)} \rightarrow \sigma^*_{C(34)-Br(43)}$	2.95	2.68
$\sigma_{C(11)-C(16)} \rightarrow \sigma^*_{C(2)-C(3)}$	2.23	1.28	$\sigma_{C(31)-H(33)} \rightarrow \sigma^*_{C(34)-C(39)}$	3.98	3.87
$\sigma_{C(11)-C(16)} \rightarrow \sigma^*_{C(2)-C(3)}$	-	2.07	$\sigma_{C(34)-C(39)} \rightarrow \sigma^*_{C(31)-H(31)}$	4.70	1.50
$\pi_{C(13)-O(14)} \rightarrow \sigma^*_{C(3)-C(11)}$	1.35	1.06	$\sigma_{C(34)-C(39)} \rightarrow \sigma^*_{C(39)-H(42)}$	-	1.05
$\sigma_{C(20)-H(22)} \rightarrow \sigma^*_{C(5)-C(6)}$	4.21	4.32	$\sigma_{C(34)-Br(43)} \rightarrow \sigma^*_{C(24)-C(31)}$	2.96	5.00
$\sigma_{C(33)-H(34)} \rightarrow \sigma^*_{C(13)-O(15)}$ ())		1.66	$\sigma_{C(34)-Br(43)} \rightarrow \sigma^*_{C(35)-H(37)}$	2.91	2.76
$\sigma_{C(33)-H(34)} \rightarrow \sigma^*_{C(13)-O(15)}$	3.99	1.09	$\sigma_{C(34)-Br(43)} \rightarrow \sigma^*_{C(39)-H(42)}$	3.97	5.00
$\sigma_{C(41)-H(32)} \rightarrow \sigma^*_{C(36)-Br(45)}$	7.12	7.27	$\sigma_{C(39)-H(42)} \rightarrow \sigma^*_{C(34)-Br(43)}$	7.12	7.31
$\eta_{2\ O(14)} \rightarrow \sigma^*_{C(11)-C(13)}$	18.35	18.96	$\eta_{1\ O(24)} \rightarrow \sigma^*_{C(23)-O(15)}$	7.52	8.61
$\eta_{2\ O(14)} \rightarrow \sigma^*_{C(13)-O(15)}$	35.37	35.37	$\eta_{1\ O(24)} \rightarrow \sigma^*_{C(31)-H(32)}$	-	2.72
$\eta_{1\ O(15)} \rightarrow \sigma^*_{C(13)-O(14)}$	7.65	8.60	$\eta_{2\ O(24)} \rightarrow \pi^*_{C(23)-O(25)}$	45.37	46.46
$\eta_{1\ O(15)} \rightarrow \sigma^*_{C(13)-H(35)}$	1.27	2.73	$\eta_{2\ O(24)} \rightarrow \sigma^*_{C(31)-H(33)}$	4.91	3.50
$\eta_{2\ O(15)} \rightarrow \pi^*_{C(13)-O(14)}$	47.53	46.35	$\eta_{2\ O(24)} \rightarrow \sigma^*_{C(31)-H(34)}$	-	3.30
$\eta_{2\ O(15)} \rightarrow \sigma^*_{C(33)-H(34)}$	4.19	3.48	$\eta_{2\ O(24)} \rightarrow \sigma^*_{C(34)-Br(43)}$	-	1.52
$\eta_{2\ O(15)} \rightarrow \sigma^*_{C(33)-H(35)}$	4.99		$\eta_{1\ O(25)} \rightarrow \sigma^*_{C(17)-C(23)}$	-	2.22
$\eta_{2\ O(15)} \rightarrow \sigma^*_{C(13)-O(14)}$	-	3.41	$\eta_{2\ O(25)} \rightarrow \sigma^*_{C(17)-C(23)}$	18.25	18.89
$\eta_{2\ O(15)} \rightarrow \pi^*_{C(36)-Br(45)}$	-	1.54	$\eta_{2\ O(25)} \rightarrow \sigma^*_{C(23)-O(24)}$	35.60	35.32
Σ (kcal.mol^{-1})	169.21	183.69	Σ (kcal.mol^{-1})	215.43	224.56

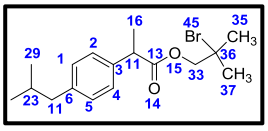

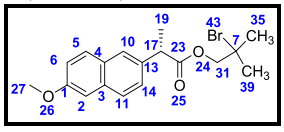

The review article by Tomasi et al. explains in a simplified and instructive manner that the factors that lead to the continuous IEF PCM are often unsuitable for certain systems [27]. The authors suggest that this may be attributed to the model's failure to consider some surface areas at specific points in the molecule, which leads to poor-precision simulation of molecular solvation. Other continuous solvation models such as PCM-SMD (*a* continuous solvation model based on the quantum mechanical charge density of the solute) afford good results for molecular solvation calculations. We believe that this model may be an alternative to better simulate the effects of solvation on the compounds evaluated herein, and it will be the subject of future study by our research group.

3.5. NBO calculations

In NBO analysis, a large *E* value indicates intensive interaction between electron donors and electron-acceptors; the possible intensive interactions are summarized in Tables 4 and 5. All electronic interactions with energy values >1 kcal.mol^{-1} were considered in the data analysis. The first important finding is that for the different conformations, the electronic interactions in the compounds surrounding the orbitals of the atoms that formed the dihedral angles α and β (α = C3-C12-C15-O16 and β = C16-C15-O16-C18) did not differ significantly based on the conformational search.

The highest-energy orbital interactions found for compounds **R1–R3** involve the aromatic ring and were not listed because high values are already expected for the orbital interactions in this region due to aromaticity.

The most significant electronic interactions are those with two pairs of electrons from the carbonyl group oxygen atom (C=O) and the adjacent oxygen in the ester group R-O-(CO). Therefore, the main interactions that stabilize the conformation of compounds **R1–R3** are $\eta_O \rightarrow \sigma^*_{C\text{-}C}$, $\eta_O \rightarrow \sigma^*_{C\text{-}O}$, $\eta_O \rightarrow \sigma^*_{C\text{-}O}$, and $\eta_O \rightarrow \pi^*_{C\text{-}O}$ (as highlighted in Tables 4 and 5).

The sum of the orbital contributions to the lowest energy (more stable) conformation is greater than that determined from the experimental and theoretical data, which enabled us to identify two conformations: the anti-clinal conformation is the preferred and lowest energy conformer (global minimum) for para-substituted 2-methyl-2-(bromo)propyl-phenyl acetate **R1** (Y = H, OMe, Cl, and NO_2), **R2**, and **R3** based on the dihedral angle between the aromatic ring and the carbonyl group.

For compounds $\mathbf{R_2}$ and $\mathbf{R_3}$ (NSAID derivatives), the $\eta_O \rightarrow \sigma^*_{C\text{-}O}$ electronic interaction was not significant. Other orbital interactions such as $\eta_O \rightarrow \pi^*_{C\text{-}O}$ were more significant than in the case of $\mathbf{R_1}$ (Y = OMe, H, and Cl), which indicates that these interactions con-

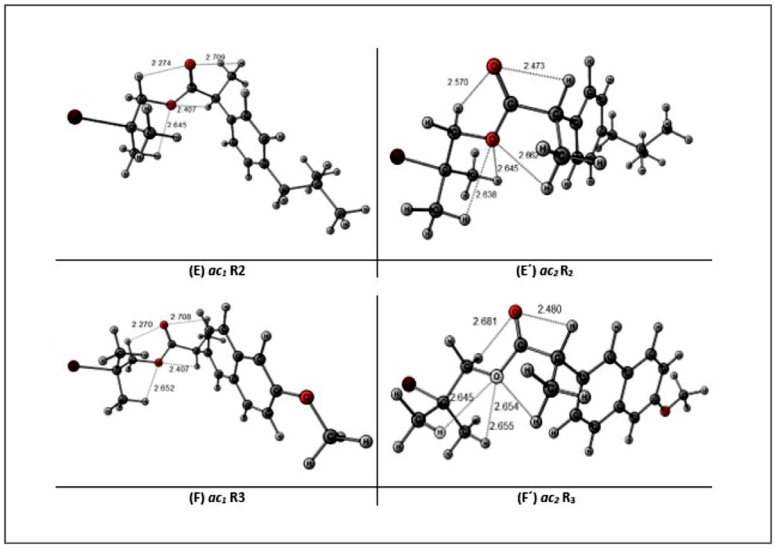

Fig. 7. Molecular graphs for the *ac* conformers of the compounds **R2** and **R3** showing electrostatic and charge transfer (intramolecular hydrogen bonds) interactions between the negative oxygen atoms in the carbonyl and the ester groups and the adjacent hydrogen atoms.

Table 6
Charge (Mulliken) (e) of selected atoms obtained at DFT-B3LYP/6-311+G (2df,2p) level for the 2-bromo-2-methylpropyl-2-aryl-acetate-*para*-substituted R1 (Y = H, OMe, Cl and NO_2), 2-bromo-2-methylpropyl 2-(4-isobutylphenyl)propanoate (derivative of Ibuprofen) R2 and 2-bromo-2-methylpropyl 2-(6-methoxynaphthalen-2-yl)propanoate (derivative of Naproxen) R3 (the minus sign indicates excess of negative charge).

Comp	Y	Conf.[a]	C1	C2	C3	O4	O5	C6	C7	Br10	C11
R_1	**OMe**	$ac_{(1)}$	0.648	-0.113	0.137	-0.338	-0.077	-0.178	0.555	-0.171	-
		$g_{(1)}$	0.756	-0.123	-0.090	-0.363	-0.042	-0.210	0.546	-0.168	-
	H	$ac_{(1)}$	0.828	-0.242	0.125	-0.337	0.075	-0.166	0.521	-0.170	
		$g_{(1)}$	0.785	-0.125	-0.086	-0.364	-0.045	-0.197	0.522	-0.166	
	Cl	$ac_{(1)}$	0.512	-0.270	0.065	-0.328	-0.070	-0.154	0.345	-0.177	-
	NO_2	$g_{(1)}$	0.755	-0.136	0.073	-0.342	-0.044	-0.248	0.484	-0.169	-
		$c_{(1)}$	0.747	0.088	-0.158	-0.348	-0.066	-0.197	0.512	-0.157	-
R_2		$ac_{(2)}$	0.454	0.583	-0.200	-0.328	-0.058	-0.173	0.573	-0.170	-0.434
		$ac_{(1)}$	0.540	0.203	-0.014	-0.325	-0.049	-0.091	0.391	-0.176	-0.484
R_3		$ac_{(2)}$	0.513	0.595	-0.114	-0.333	-0.062	-0.158	-0.531	-0.171	-0.447
		$ac_{(1)}$	0.643	0.481	-0.108	-0.334	-0.056	-0.099	0.396	-0.179	-0.447

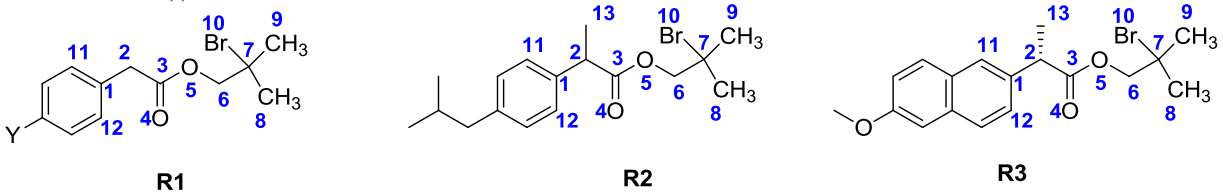

tribute the most to stabilizing the compound. The sum of all orbital interactions between the more and less stable conformers was 14.48 and 9.13 kcal.mol^{-1} for $\mathbf{R_2}$ and $\mathbf{R_3}$, respectively.

The increased electron density at the oxygen atoms leads to elongation of the respective bond lengths and a lowering of the corresponding stretching wave number. The electron density is transferred from the $n_{(O)}$ to the anti-bonding π orbital of the bonds. The hyper-conjugative interaction energy was deduced from the second-order perturbation approach. The delocalization of the electron density between occupied Lewis-type (bond or lone pair) NBO orbitals and formally unoccupied (anti-bonding) non-Lewis NBO orbitals corresponds to a stabilizing donor–acceptor interaction. Hence, the title compound is stabilized by these orbital interactions (Table 5).

Table 6 shows selected interatomic distances and the sum of the corresponding van der Waals radii of the involved atoms (the value is calculated as the sum of the difference in the van der Waals radius minus the distance between the two corresponding atoms). Table 7 shows the atomic charge of each atom in the **R1–R3** conformers.

The data in Tables 6 and 7 show that for the lowest energy and most stable **R1** (Y = H, OMe, Cl, and NO_2) conformers, there are four electrostatic and charge-transfer interactions (intramolecular hydrogen bonds) that contribute to the stability of the conformers; for the higher-energy conformations, only three interactions were observed (Fig. 6).

For compounds **R2** (an ibuprofen derivative) and **R3** (a naproxen derivative), five interactions were observed for the highest energy anti-clinal (ac_2) conformer and four interactions for the lowest energy anti-clinal (ac_1) conformer (Fig. 7). The low-energy anti-clinal (ac_1) conformers of compounds **R2** and **R3** exhibit a strong interaction between O4•••H6, indicative of a strong charge-transfer process, which may justify the lower number of interactions observed for these compounds (Table 7).

Table 7
Selected Interatomic Distances (Å) (intramolecular hydrogen bonds) at DFT/6-311+G (2df.2p) level of 2-bromo-2-methylpropyl-2-aryl-acetate-*para*-substituted R1(X = H, OMe, Cl and NO_2), 2-bromo-2-methylpropyl 2-(4-isobutylphenyl)propanoate (derivative of Ibuprofen) R2 and 2-bromo-2-methylpropyl 2-(6-methoxynaphthalen-2-yl)propanoate (derivative of Naproxen) R3 (sum of van der Waals radii = 2.72 Å).

Comp.	Y	Conf.	A $O_4...H_2$	A' ΔI	B $O_4...H_6$	B' ΔI	C $O_4...H_{11}$	C' ΔI	D $O_4...H_{12}$	D' ΔI	E $O_5...H_2$	E' ΔI	F $O_5...H_8$	F' ΔI	G $O_5...H_9$	G' ΔI	H $O_4...H_{11}$	H' ΔI
R_1	**OMe**	$ac_{(1)}$	2.55	0.17	2.27	0.45	-	-	3.19	-0.47	2.48	0.24	2.65	0.07	2.74	-0.02	-	-
		$g_{(1)}$	2.86	-0.14	2.26	0.46	-	-	2.88	-0.16	2.39	0.33	2.66	0.06	2.73	-0.01	-	-
	H	$ac_{(1)}$	2.55	0.17	2.28	0.44	-	-	3.11	-0.39	2.48	0.24	2.65	0.07	2.74	-0.02	-	-
		$g_{(1)}$	2.85	-0.13	2.26	0.46	-	-	2.82	-0.1	2.38	0.34	2.66	0.06	2.74	-0.02	-	-
	Cl	$ac_{(1)}$	2.56	0.16	2.59	0.13	-	-	3.02	-0.3	2.48	0.24	2.64	0.08	2.63	0.09	-	-
	NO_2	$g_{(1)}$	2.50	0.22	2.61/2.65	0.44/0.43	-	-	3.32	-0.6	2.45	0.27	2.57	0.15	-	-	-	-
		$c_{(1)}$	2.95	-0.23	2.28	0.15	-	-	2.92	-0.2	2.42	0.3	2.66	0.06	2.74	-0.02	-	-
R_2	**Ibuprofen**	$ac_{(1)}$	3.20	-0.48	2.27	0.45	2.70	0.02	2.81	-0.09	2.40	0.32	2.73	-0.01	2.64	0.08	3.79	-1.07
		$ac_{(2)}$	2.47	0.25	2.57	0.15	3.49	-0.77	3.52	-0.8	3.25	-0.53	2.63	0.09	2.64	0.08	2.66	0.06
R_2	**Naproxen**	$ac_{(1)}$	3.20	-0.48	2.27	0.45	2.70	0.02	2.81	-0.09	2.40	0.32	2.73	-0.01	2.65	0.07	3.78	-1.06
		$ac_{(2)}$	2.47	0.25	2.68	0.04	3.62	-0.9	3.74	-1.02	3.23	-0.51	2.65	0.07	2.65	0.07	2.65	0.07

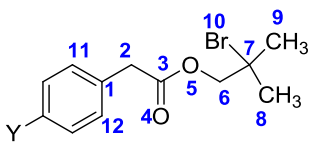

R1

Y = CH_3O, H, Cl. NO_2

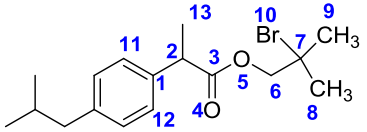

R2

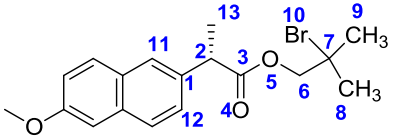

R3

The preference for the *anti*-conformation between the bromo and ester-oxygen atom [φ = O(5)-C(6)-C(7)-Br(10)] (Table 2) is consistent with the expectations from the stronger H-bonds, O(5)•••H8 and O(5) ••H9 (Table 6), of the methyl groups. Another strong intermolecular hyper-conjugative interaction that stabilizes the *gauche* conformation $\sigma_{C(CH3)}$-$H_{(CH3)} \rightarrow \sigma^*_{C\text{-}Br}$ is also operative.

The calculations indicate that these interactions are important because they decrease the strength of the C–Br bond and justify the high positive charge on the carbon atom and negative charge on the Br atom, which weakens this bond. Thus, we can infer that these compounds are excellent precursors for the synthesis of derivatives via unimolecular nucleophilic S_N1 reactions with the formation of carbocations.

4. Conclusion

Experimental and theoretical analyses enabled us to identify two conformations of *para*–substituted 2-bromo-2-propyl 2-phenylacetate (Y = H, OMe, Cl and NO_2) (**R1**), ibuprofen (**R2**), and naproxen (**R3**) analogs. The preferred and lowest-energy conformer (global minimum) is the *anti-clinal* geometry based on the dihedral angle between the aromatic ring and carbonyl group (α), and the second stable conformation presented a preferential *cis* geometry.

Solvation calculations using IEF PCM failed to accurately describe the experimental data, but the trends were very similar to those of the experimental results. We believe that the use of other solvation calculation methods, such as PCM-SMD or even IEF PCM, which specifies the solvent molecule in the starting geometry, may lead to more satisfactory results.

The NBO analysis showed that the $\eta_O \rightarrow \sigma^*_{C\text{-}O}$ electronic interaction for compounds **R2** and $\mathbf{R_3}$ (NSAID derivatives) was not as significant as it was for compound **R1** (Y = OMe, H, Cl and NO_2). The $\eta_O \rightarrow \pi^*_{C\text{-}O}$ orbital interactions are more significant than in the case of $\mathbf{R_1}$, which indicates the higher contribution of these interactions to stabilizing compounds $\mathbf{R_2}$ and $\mathbf{R_3}$.

These compounds preferentially adopt the *anti*-conformation between the bromo and ester-oxygen atom, which is stabilized by strong intermolecular hyper-conjugative $\sigma_{C(CH3)}$-$H_{(CH3)} \rightarrow \sigma^*_{C\text{-}Br}$ interactions.

Declaration of Competing Interest

All authors declare no conflict of interest.

Acknowledgment

The authors thank Fundação de Amparo à Pesquisa do Estado de São Paulo (FAPESP - Grant Numbers: 2010/51784-3 and 2013/16644-4) for financial support. The authors also thank Coordenação Nacional de Aperfeiçoamento do Ensino Superior (CAPES - Brazil) for the research fellowships granted to D.C.S and M.M.R. Professor Paulo Roberto Olivato is gratefully acknowledged for providing laboratory facilities.

Supplementary materials

Supplementary material associated with this article can be found, in the online version, at doi:10.1016/j.molstruc.2021.130027.

References

[1] N.D. Yeomans, et al., N. Engl. J. Med. 338 (1998) 719–726.
[2] C.J Hawkey, et al., N. Engl. J. Med. 338 (1998) 727–734.
[3] C. Bombardier, et al., N. Engl. J. Med. 23 (2000) 1520–1528.
[4] S.N. Elliott, W. Mcknight, G. Cirino, J.L. Wallace, Gastroenterology 109 (1995) 524–530.
[5] S. Fiorucci, E. Antonelli, J.L. Burgaud, A. Morelli, Drug Saf. 24 (2001) 801–811.
[6] J.L. Wallace, L.J. Ignarro, S. Fiorucci, Nat. Rev. Drug Discov. 1 (2002) 375–382.
[7] S. Fiorucci, P. Del Soldato, Dig. Liver Dis. 35 (2003) S9–19.
[8] S. Fiorucci, E. Antonelli, Curr. Top. Med. Chem. 5 (2005) 487–492.
[9] A.R. Butler, P. Rhodes, Anal. Biochem. 249 (1997) 1–9.
[10] J.L. Wallace, B. Reuter, C. Cicala, W. McKnight, M.B. Grisham, G. Cirino, Gastroenterology 107 (1994) 173–179.
[11] S.W. Tam, et al., J. Med Chem. 43 (2000) 4005–4016.
[12] G.A. Balint, Trends Pharmacol. Sci. 19 (1998) 401–403.
[13] P. Kubes, J.L. Wallace, Mediators Inflamm. 4 (1995) 397–405.
[14] S. Somasundaram, et al., Gut 40 (1997) 608–613.
[15] I.A. Siddiqui, A. Malik, V.M. Adhami, M.B. Asim, B.S. Sarfaraz, H. Mukhtar, Oncogene 27 (2008) 2055–2063.
[16] J. Loscalzo, D. Smick, N. Andon, J. Cooke, J. Pharmaco. Exp Ther. 249 (1989) 726–729.
[17] M.M. Reginato, D.R. Paiva, F.R. Sensato, H.P. Monteiro, A.K.C.A. Reis, Spectrochim. Acta A Mol. Biomol. Spectrosc. 207 (2019) 132–142.
[18] M. Liras, J.M. García-García,, I. Quijada-Garrido, A. Gallardo, R. París, Macromolecules 44 (10) (2011) 3739–3745.
[19] Galactic Industries Corporation, Salem, NH, USA, 1991−1998.
[20] M.J. Frisch, G.W. Trucks, H.B. Schlegel, G.E. Scuseria, M.A. Robb, J.R. Cheeseman, G. Scalmani, V. Barone, B. Mennucci, G.A. Petersson, H. Nakatsuji, M. Caricato, X. Li, H.P. Hratchian, A.F. Izmaylov, J. Bloino, G. Zheng, J.L. Sonnenberg, M. Hada, M. Ehara, K. Toyota, R. Fukuda, J. Hasegawa, M. Ishida, T. Nakajima, Y. Honda, O. Kitao, H. Nakai, T. Vreven, J.A. Montgomery Jr., J.E. Peralta, F. Ogliaro, M.J. Bearpark, J. Heyd, E.N. Brothers, K.N. Kudin, V.N. Staroverov, R. Kobayashi, J. Normand, K. Raghavachari, A.P. Rendell, J.C. Burant, S.S. Iyengar, J. Tomasi, M. Cossi, N. Rega, N.J. Millam, M. Klene, J.E. Knox, J.B. Cross, V. Bakken, C. Adamo, J. Jaramillo, R. Gomperts, R.E. Stratmann, O. Yazyev, A.J. Austin, R. Cammi, C. Pomelli, J.W. Ochterski, R.L. Martin, K. Morokuma, V.G. Zakrzewski, G.A. Voth, P. Salvador, J.J. Dannenberg, S. Dapprich, A.D. Daniels, Ö. Farkas, J.B. Foresman, J.V. Ortiz, J. Cioslowski, D.J. Fox, Gaussian 09, Gaussian, Inc., Wallingford, CT, USA, 2009.
[21] K. Roy, M. Todd, Shawnee Mission, K. GaussView, Version 5, John. Semichem Inc., Dennington, 2009.
[22] D.A. Zhurko, G.A.Z. Chemcraft, 2014.
[23] C. Lee, C. Hill, N. Carolina, Phys. Rev. 37 (1988) 785–789.
[24] A.D. Becke, J. Chem. Phys. 98 (1993) 5648–5652.
[25] S.H. Vosko, L. Wilk, M. Nusair, Can. J. Phys. 58 (1980) 1200–1211.
[26] A.E. Reed, F. Weinhold, J. Chem. Phys. 83 (1985) 1736–1740.
[27] J. Tomasi, B. Mennucci, R. Cammi, Chem. Rev. 105 (2005) 2999–3093.